Homogenization of Two-Dimensional Clusters of Rigid Rods in Air

Daniel Torrent, Andreas Håkansson, Francisco Cervera, and José Sánchez-Dehesa*

Wave Phenomena Group, Nanophotonics Technology Center, Polytechnic University of Valencia, C/Camino de Vera s/n, E-46022 Valencia, Spain

(Received 16 November 2005; revised manuscript received 8 February 2006; published 22 May 2006)

The scattering of sound waves by circular-shaped clusters consisting of two-dimensional distributions of rigid cylinders in air is studied in the low-frequency limit (homogenization) both theoretically and experimentally. Analytical formulas for the effective density and sound speed are obtained in the framework of multiple scattering. Here, an experimental demonstration is reported in which a cluster of wooden rods acoustically behaves as a cylinder of argon gas. Moreover, evidence is presented indicating the validity of the homogenization in this cluster at frequencies lower than 3 kHz, which corresponds to a wavelength that is only 4 times the parameter of the embedded lattice and is a quarter of the cluster's diameter.

DOI: 10.1103/PhysRevLett.96.204302 PACS numbers: 43.20.+g, 43.40.+s

Recently, there has been a great interest in studying the properties of sonic crystals, a name that specifically defines periodic distributions of sound scatterers in air. Their properties in the low-frequency limit have been studied by several groups [1–6] for its possible use as refractive devices. A key problem of these systems has become the calculation of the homogenized parameters controlling their refractive properties; i.e., their effective sound velocity (c_{eff}) and density (ρ_{eff}). Another issue of great interest is to determine the cluster's minimum size in which the refractive effects dominate over the diffractive. In this regard, a controversy has recently been raised about whether the sound focusing produced by lenticular-shaped clusters is mainly due to refraction instead of diffraction [1,3,7,8]. Meanwhile, the work by Kuo and Ye [9] predicted that focusing effects by large enough clusters of two-dimensional (2D) scatterers can be well described by lensmaker's formula, and recently the refraction of water waves by periodic cylinders arrays has been studied in the long wavelength limit [10].

In this Letter an analytical theory based on the multiple scattering method is developed and applied to study the homogenization of circular-shaped clusters made of 2D periodic distribution of rigid scatterers in air. We have obtained compact formulas for ρ_{eff} and c_{eff} that take into account the inner structure of the periodic medium. In comparison with previous work [5], our approach gives not only c_{eff} but also ρ_{eff} and is able to determine the critical ratio between the cluster's size and the wavelength allowing the homogenization. Measurements made on a sample consisting of wooden cylinders in air support the validity of our formulas. Particularly, experimental results indicate that sound scattering by the studied cluster is well described by a single gas cylinder for wavelengths larger than one-forth of the cluster's diameter.

Let us consider a cluster made of a 2D arrangement of rigid cylinders (made of material A) embedded in a fluid or gas background made of material B. Without losing generality we assume hereafter air for material B. Here, in order to find the appropriate effective acoustic parameters we focus on the behavior of this structure in the long wavelength limit. Hereafter, we will use an overline over a variable to denote the corresponding quantity in the effective medium normalized to the corresponding magnitudes of material B; i.e., $\bar{\rho} = \rho/\rho_b$ and $\bar{c} = c/c_b$. As it turns out, when the wavelength increases, the scattering properties of the cluster asymptotically approach those of an uniform cylinder of diameter D and with a single defined density $\bar{\rho}_{\text{eff}}$ and sound velocity $\bar{c}_{\text{eff}}$. We first give an heuristic derivation to establish this connection.

If an external sound wave P^{ext} with temporal dependence $e^{-i\omega t}$ impinges a cluster of N cylinders located at positions $\vec{R}_\alpha$ ($\alpha = 1, 2, \ldots, N$), the scattered field at a given position of polar coordinates (r, θ) is [4,11]

$$P^{\text{sca}}(r, \theta, \nu) = \sum_{\alpha=1}^{N} \sum_{s=-\infty}^{s=+\infty} (A_\alpha)_s H_s(kr_\alpha) e^{is\theta_\alpha}, \qquad (1)$$

where H_s is the sth order Hankel function of the first kind, and $(r_\alpha, \theta_\alpha)$ are the polar coordinates of the α cylinder in a reference frame centered at the cylinder. Here, $k = \omega/c_b$, $\nu = \omega/2\pi$, and $(A_\alpha)_s$ are the coefficients to be determined.

By using Graff's theorem, the expression above can be cast into an expression that is equivalent to the scattered pressure by a single cylinder (SC) located at the origin:

$$P^{\text{sca}}(r, \theta, \nu) = \sum_{q=-\infty}^{q=+\infty} A_q^{\text{SC}} H_q(kr) e^{iq\theta}, \qquad (2)$$

where

$$A_q^{\text{SC}} \equiv \sum_{\alpha=1}^{N} \sum_{s=-\infty}^{s=+\infty} (A_\alpha)_s (J_\alpha)_{qs}, \qquad (3)$$

being $(J_\alpha)_{qs} \equiv J_{q-s}(kR_\alpha) e^{i(s-q)\Phi_\alpha}$.

By truncating the angular momentum within $|s| \leq s_{\max}$ and $|q| \leq q_{\max}$, the last equation reduces to a linear equation. In matrix form, $\mathcal{A}^{\mathcal{SC}} = \mathcal{J}\mathcal{A}$, where $\mathcal{A}^{\mathcal{SC}}$ and $\mathcal{A}$ are column matrices and $\mathcal{J}$ is a N-element vector where each element is a rectangular matrix of dimension $(2q_{\max} + 1) \times (2s_{\max} + 1)$. Also, it is known that $\mathcal{A} = \mathcal{M}^{-1}\mathcal{S}$

[4], where $\mathcal{M}$ is a square matrix and $\mathcal{S}$ is a matrix of coefficients that define the external wave through the relationship $\mathcal{S} = \mathcal{T}\tilde{\mathcal{J}}\mathcal{A}^0$, where $\mathcal{T}$ is the T matrix of a single cylinder, $\tilde{\mathcal{J}}$ has matrix elements $(\tilde{J}_\alpha)_{qs} = J_{s-q}(kR_\alpha) \times e^{i(s-q)\Phi_\alpha}$, and $\mathcal{A}^0$ is the matrix defining the coefficient of the external wave impinging the cluster. Finally, we arrive to the following matrix expression:

$$\mathcal{A}^{\mathrm{SC}} = \mathcal{J}\mathcal{M}^{-1}\mathcal{T}\tilde{\mathcal{J}}\mathcal{A}^0 \equiv \mathcal{T}_{\mathrm{eff}}(\nu)\mathcal{A}^0, \qquad (4)$$

which defines the effective T matrix of the cluster treated as a single cylinder.

For the case of large wavelengths and for a wide range of filling fractions (f), it is possible to demonstrate that [12] $\lim_{k\to 0}\mathcal{M}^{-1} = \mathcal{I}$ and $\lim_{k\to 0}\mathcal{J}_\alpha = \lim_{k\to 0}\tilde{\mathcal{J}}_\alpha = \mathcal{I}_\alpha$, where $\mathcal{I}$ and $\mathcal{I}_\alpha$ are identity matrices. Therefore, the nondiagonal terms of $\mathcal{T}_{\mathrm{eff}}(\nu)$ go to zero in the limit $k \to 0$ because of the circular symmetry of the cluster, and the diagonal terms, $(T_{\mathrm{eff}})_q$, have a dependence k^{2q}, if $q \neq 0$. For case $q = 0$, $(T_{\mathrm{eff}})_0 \propto k^2$. Therefore, the following relationships are found for the lower order terms:

$$\lim_{k\to 0}\frac{(T_{\mathrm{eff}})_0}{k^2} = N\lim_{k\to 0}\frac{T_0}{k^2}, \qquad (5)$$

$$\lim_{k\to 0}\frac{(T_{\mathrm{eff}})_1}{k^2} = N\lim_{k\to 0}\frac{T_1}{k^2}, \qquad (6)$$

where $T_0 \equiv T_{00}$ and $T_1 \equiv T_{11}$ are the first elements of the diagonal T matrix for an uniform cylinder with radius $d/2$, density $\bar{\rho}$, and sound velocity $\bar{c}$ matrix [13]:

$$T_{qq}(\nu) = -\frac{\bar{\rho}_q J_q'(kd/2) - J_q(kd/2)}{\bar{\rho}_q H_q'(kd/2) - H_q(kd/2)},$$
$$\text{where } \bar{\rho}_q(\nu) \equiv \bar{\rho}\,\bar{c}\,\frac{J_q(kd/2/\bar{c})}{J_q'(kd/2/\bar{c})}. \qquad (7)$$

The behavior of the T_0 and T_1 terms are easily obtained in the large wavelength limit, and Eqs. (5) and (6) can be cast in the following relationships:

$$\lim_{k\to 0}\frac{(T_{\mathrm{eff}})_0}{k^2} = \frac{i\pi D^2}{16}\left[\frac{1}{\bar{\rho}_{\mathrm{eff}}\bar{c}_{\mathrm{eff}}^2} - 1\right], \qquad (8)$$

$$\lim_{k\to 0}\frac{(T_{\mathrm{eff}})_1}{k^2} = \frac{i\pi D^2}{16}\,\frac{\bar{\rho}_{\mathrm{eff}} - 1}{\bar{\rho}_{\mathrm{eff}} + 1}. \qquad (9)$$

These equations define a numerical procedure to get the homogenization parameters of a N-cylinders' cluster with diameter D. But more important, since $P^{\mathrm{sca}}(r, \theta, \nu)$ is measurable, Eq. (4) allows the empirical determination of the effective T matrix, which used in conjunction with Eqs. (8) and (9) define an experimental approach to determine the homogenized parameters in the long wavelength limit provided that D is known. Here, since we have been working with hexagonal arrangements of cylinders, $D = (2N\sqrt{3}/\pi)^{1/2}a$ [so that $\frac{N\pi(d/2)^2}{\pi(D/2)^2}$ equals the filling fraction of hexagonal lattice $f = \frac{\pi}{2\sqrt{3}}(d/a)^2$, where a is the lattice parameter].

Figure 1 plots the values obtained as a function of f by multiple scattering simulation using the approach of rigid cylinders. It is noteworthy that, regarding the effective sound speed, our modeling fairly agrees (in the full range of f) with the exact theory of Ref. [5], where homogenization of an infinite periodic system was studied by using a plane waves expansion. However, now our approach is also able to obtain the density of effective medium.

The homogenized parameters at low enough f can be analytically obtained, and they are

$$\bar{\rho}_{\mathrm{eff}} = (1 + f)/(1 - f), \qquad \bar{c}_{\mathrm{eff}} = 1/\sqrt{1 + f}. \qquad (10)$$

On one hand, these expressions recover the formula derived by Barryman [14] for the effective mass density, and on the other hand, the effective sound velocity coincides with the heuristic model reported in Ref. [1]. Both results have been recently corroborated by a multiple scattering approach applied to an infinite system [15]. Expressions similar to that in Eq. (10) were also obtained for the case of cylinders of finite density ρ_{cyl} and sound velocity v_{cyl} [16]. However, here results are presented under the simplified approach of rigid cylinders (infinite density) because the majority of solids have densities much larger than that of air, and, therefore, the huge mismatch impedance forbids the penetration of sound waves into the cylinder. For lighter materials new expressions have to be found taking into account their exact density and the velocities of the different waves propagating inside the cylinder. Also note that relationships in Eq. (10) have appeared in studying water waves, where homogenization was performed in the framework of the coherent-potential-approximation [10].

Experimentally, the model of homogenization has been verified by analyzing a circular-shaped cluster made of 151

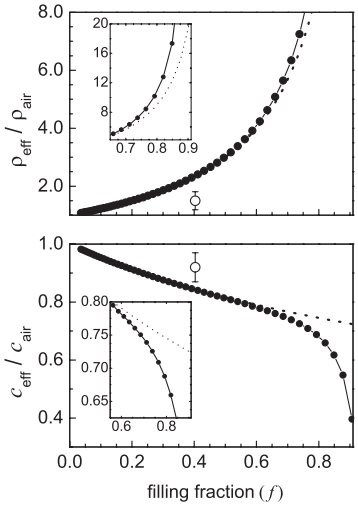

FIG. 1. Homogenized parameters for a circular-shaped cluster made of 151 cylinders put in a hexagonal lattice. Black dots represent the multiple scattering simulations. The dashed lines define values obtained by analytical formulas in Eq. (10). The open circles with error bars represent the experimental results.

wooden cylinders 1 m long and radius 1 cm arranged in an hexagonal distribution with $a = 3$ cm ($f = 0.40$). Measurements have been performed in an echo-free chamber as follows. A white sound generated by an acoustic column speaker within a wide range of frequencies was employed as incident sound. Pressure maps were obtained by a set of two microphones. The first microphone was located at a distance $r_0 = 170$ cm from the center of the cluster, hanging from a robotic arm that allows its movement on the polar angle θ, and it is computer controlled using a stepper motor within a maximum resolution of 1° per step. The second microphone was fixed at approximately 2.2 m from the loudspeaker, and it was used as a reference to get the phase of the pressure. Pressure measurements are automatically taken by means of a two channel fast-Fourier transform dynamic signal analyzer board, type NI-4551B. Both the cross spectrum and the auto spectra were simultaneously obtained at each θ_i.

A total of 256 spectra have been taken to generate the averaged spectrum finally assigned to θ_i. Thus, for a given frequency, the root-mean-square (rms) pressure $P_{\mathrm{rms}}(r_0, \theta_i)$ is obtained. Pressure maps are obtained with a resolution of 10 Hz in ν and 2° in θ. The total time elapsed to get a pressure map is about 3 h. Two separated measurements were performed. The one without sample allows one to obtain the sound pressure of the external beam, $P^{\mathrm{ext}}_{\mathrm{rms}}(r_o, \theta, \nu)$. Here, the sound amplification (SA) along the circle surrounding the sample will be presented:

$$\mathrm{SA}\,(r_0, \theta, \nu)(\mathrm{dB}) = 20\log_{10}\left(\frac{|P_{\mathrm{rms}}(r_0, \theta, \nu)|}{|P^{\mathrm{ext}}_{\mathrm{rms}}(r_0, \theta, \nu)|}\right). \qquad (11)$$

Figures 2(a) and 2(b) plot the SA maps corresponding to the two high symmetry directions of the hexagonal lattice ΓX and ΓJ, respectively, with respect to the impinging wave. Only angles $0° \leq \theta \leq 180°$ are represented because of the mirror symmetry of the problem. Three main phenomena are noticeable in these maps. First, both maps show a wavy background that is produced by the interference between incident and scattered waves. Second, at large enough frequencies, SAs are shown along certain directions that are related to diffraction effects produced by lattice planes. For example, sound amplification at backscattering ($\theta = 180°$) is observed in Fig. 2(a) in the region enclosed by the horizontal lines. This feature defines the pseudogap produced at these frequencies by the planes (10) of the crystal lattice. Third, for large enough wavelengths the sound cannot distinguish the inner structure of the cluster, and consequently, the map obtained for the cluster oriented along the ΓX direction is the same as that obtained along the ΓJ orientation. This is the effect concerning this work. To determine the cutoff frequency (ν_c) under the one where this phenomenon appears, we have analyzed the difference between those maps.

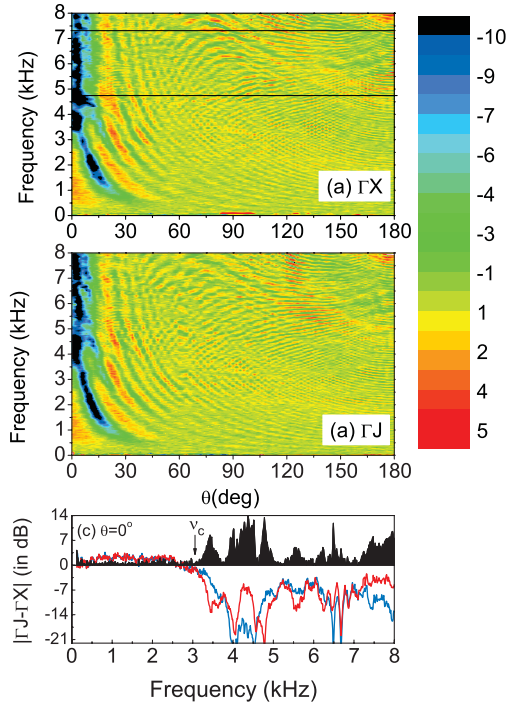

FIG. 2 (color). (a) Sound amplification map SA(ν, θ_i) measured at 170 cm around the center of the cluster for the case in which the external sound wave impinging the hexagonal lattice is oriented along the ΓX direction. The horizontal lines define the bottom (4.6 kHz) and top (7.1 kHz) edges of the pseudogap associated with the acoustic crystal embedded in the cluster. (b) The corresponding map taken when the cluster is oriented along the ΓJ direction. (c) Difference (in dB) of sound pressures measured along the two high symmetry directions at forward scattering, $\theta = 0°$. The SAs along ΓX and ΓJ are represented by the red and blue lines, respectively.

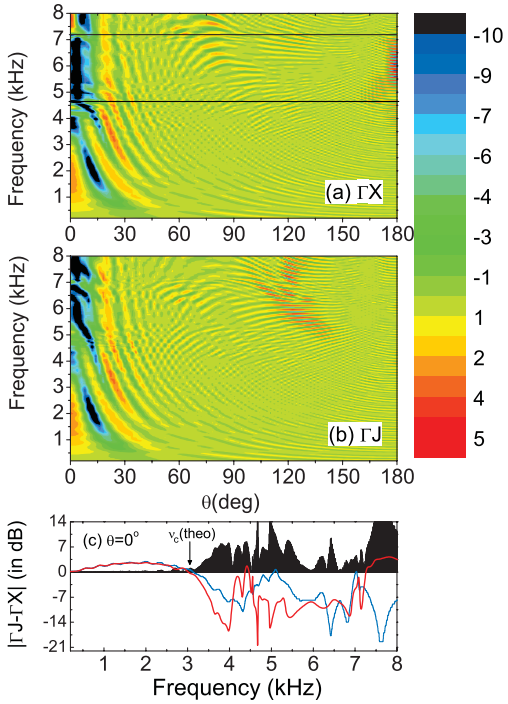

FIG. 3 (color). The corresponding sound amplification maps obtained by multiple scattering theory applied to the cluster experimentally studied in Fig. 2.

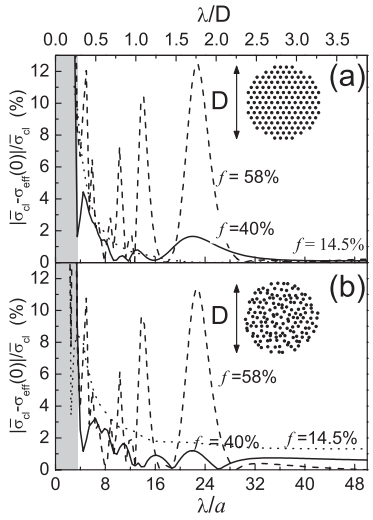

FIG. 4. Relative difference between the forward scattering cross section calculated for a cluster of cylinders $[\bar{\sigma}_{\mathrm{cl}}]$ and its corresponding homogenized cylinder $[\sigma_{\mathrm{eff}}(0)]$, with diameter D. Three filling fractions are reported: $f = 0.145$ (dotted lines), $f = 0.40$ (continuous line), and $f = 0.58$ (dashed lines). The shadowed region defines those wavelengths below the homogenization limit for the cluster experimentally studied in Fig. 2 (i.e., $\lambda \leq \lambda_c \approx 4a$). (a) Results for an hexagonal cluster. (b) Results obtained by averaging ten different weak-disordered arrangements of cylinders within the circle D.

Particularly, Fig. 2(c) shows that below $\nu_c \approx 3$ kHz both maps are practically equal.

A multiple scattering simulation [4] of the cluster experimentally studied has been performed by considering an impinging wave generated by a punctual sound source placed at the position of the loudspeaker. The calculated maps are shown in Figs. 3(a) and 3(b). Figure 3(c) plots the SAs along the two high symmetry directions and their absolute difference at $\theta = 0°$. These last results show that the cutoff frequency of homogenization $[\nu_c(\mathrm{theo})]$ is also 3 kHz, as is the one experimentally determined. The agreement between theoretical simulations and experimental measurements is remarkable at any angle for frequencies below 3 kHz. This agreement let us to conclude that homogenization of clusters is valid at wavelength λ_c as low as a fourth of the cluster's diameter, which supports the claim made in Ref. [1].

To more deeply analyze the homogenization approach, we calculated the differential scattering cross section, $\sigma(\theta)$. After averaging the forward scattering for different orientations, φ, of the cluster, $\bar{\sigma}_{\mathrm{cl}} = \frac{1}{2\pi}\int_0^{2\pi}\sigma_\varphi(0)d\varphi$, we have compared it with the uniform cylinder case, $\sigma_{\mathrm{eff}}(0)$. Their relative difference (in percentage) is plotted in Fig. 4(a) as a function of wavelength for three different filling fractions. The one corresponding to the case experimentally studied (continuous line) indicates that a maximum error of 4% is achieved for wavelengths above $\lambda_c \approx 4a$. Also, we have analyzed the robustness of the homogenization against "weak disorder" [17] in the cluster, and results are represented in Fig. 4(b). For each f the results are averaged over ten different configurations, the standard deviation being negligible. It can be concluded that under a small amount of disorder, the effective parameters of the disordered system differ only slightly from those of the perfect ordered system.

The parameters of the homogenized cluster experimentally determined from Eqs. (8) and (9) are represented in Fig. 1. They have been obtained by considering $D = 39$ cm, which has been established from the condition of f conservation. In absolute units, $\rho_{\mathrm{eff}} = 1.92 \pm 0.40\ \mathrm{kg\,m^{-3}}$ and $c_{\mathrm{eff}} = 316 \pm 17\ \mathrm{m\,s^{-1}}$, which roughly corresponds to those of argon gas ($\rho_{\mathrm{Ar}} = 1.6\ \mathrm{kg\,m^{-3}}$; $c_{\mathrm{Ar}} = 319\ \mathrm{m\,s^{-1}}$ at 25 °C). The measured parameters are slightly different to those predicted by simulations because (i) the cylinders are not long enough for the large wavelengths in which we are dealing with, and (ii) the experimental setup contains some unavoidable scattering centers that are sources of error in the data analysis.

Work supported by the Spanish Ministry of Science and Education (MEC) under Project No. TEC2004-03545. D. T. acknowledges a Ph.D. grant paid by MEC. The technical facilities provided by the group ACARMA at UPV are also acknowledged. We thank Yu. A. Kosevich for his critical reading of the manuscript.

*Corresponding author.
Electronic address: jsdehesa@upvnet.upv.es

[1] F. Cervera *et al.*, Phys. Rev. Lett. **88**, 023902 (2002).
[2] B. C. Gupta and Z. Ye, Phys. Rev. E **67**, 036603 (2003).
[3] N. Garcia, M. Nieto-Vesperinas, E. V. Ponizovskaya, and M. Torres, Phys. Rev. E **67**, 046606 (2003).
[4] L. Sanchis, A. Håkansson, F. Cervera, and J. Sánchez-Dehesa, Phys. Rev. B **67**, 035422 (2003).
[5] A. A. Krokhin, J. Arriaga, and L. N. Gumen, Phys. Rev. Lett. **91**, 264302 (2003).
[6] Z. Hou, F. Wu, X. Fu, and Y. Liu, Phys. Rev. E **71**, 037604 (2005).
[7] A. Håkansson *et al.*, Phys. Rev. E **71**, 018601 (2005).
[8] N. Garcia, M. Nieto-Vesperinas, E. V. Ponizovskaya, and M. Torres, Phys. Rev. E **71**, 018602 (2005).
[9] C. Kuo and Z. Ye, J. Phys. D **37**, 2155 (2004).
[10] X. Hu and C. T. Chan, Phys. Rev. Lett. **95**, 154501 (2005).
[11] L.-M. Li and Z.-Q. Zhang, Phys. Rev. B **58**, 9587 (1998).
[12] D. Torrent *et al.* (unpublished).
[13] Y. Y. Chen and Z. Ye, Phys. Rev. E **64**, 036616 (2001).
[14] J. G. Barryman, J. Acoust. Soc. Am. **68**, 1809 (1980); **68**, 1820 (1980).
[15] J. Mei, Z. Liu, W. Wen, and P. Sheng, Phys. Rev. Lett. **96**, 024301 (2006).
[16] From Eqs. (8) and (9) the relationships $1/\bar{c}_{\mathrm{eff}}\bar{v}^2_{\mathrm{eff}} = f/\bar{c}_{\mathrm{cyl}}\bar{v}^2_{\mathrm{cyl}} + (1-f)$ and $\bar{\rho}_{\mathrm{eff}} = [\bar{\rho}_{\mathrm{cyl}}(1+f) + (1-f)]/[\bar{\rho}_{\mathrm{cyl}}(1-f) + (1+f)]$ are obtained, respectively.
[17] The embedded lattice is maintained, but the cylinder inside each unit cell is put randomly.